JACS
JOURNAL OF THE AMERICAN CHEMICAL SOCIETY

Article

pubs.acs.org/JACS

Suppression of Hydrogen Evolution by Oxygen Reduction in Nanoporous Electrocatalysts

Ellen E. Benn,[†] Bernard Gaskey,[†] and Jonah D. Erlebacher*[,†]

[†]Department of Materials Science and Engineering, Johns Hopkins University, Baltimore, Maryland 21218, United States

ABSTRACT: Electroreduction of small molecules in aqueous solution often competes with the hydrogen evolution reaction (HER), especially if the reaction is driven even moderately hard using a large overpotential. Here, the oxygen reduction reaction (ORR) was studied under proton diffusion-limited conditions in slightly acidic electrolytes: a model system to study the relative transport kinetics of protons and reactants to an electrocatalyst and the relationship between transport and catalytic performance. Using dealloyed nanoporous nickel−platinum (np-NiPt) electrodes, we find the hydrogen evolution reaction can be completely suppressed even at high overpotentials (−400 mV vs RHE). In addition, the mechanism of oxygen reduction can be changed by using buffered versus unbuffered solutions, suggesting the reaction selectivity is associated with a transient rise (or lack thereof) in the interface pH at the np-NiPt surface. Independently controlling reactant transport to electrocatalyst surfaces at high overpotentials exhibited a surprisingly rich phenomenology that may offer a generalizable strategy to increase activity and selectivity during electroreduction reactions.

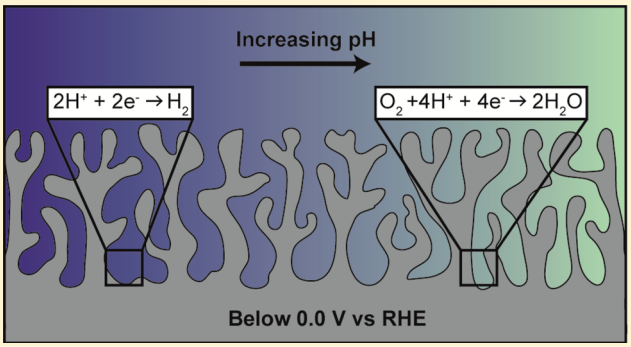

INTRODUCTION

Dealloyed nanoporous metals provide a promising platform for electrocatalysis due to a unique combination of facile synthesis and high activities.[1,2] If specific surface area alone determined a catalyst's activity, dealloying would be limited to a processing tool to fabricate roughened metal surfaces. However, there is growing recognition that nanoporosity itself leads to behavior that can enhance overall activity in electrocatalysis due to the intrinsic structural features of dealloyed metal materials. For instance, nanoporous nickel platinum (np-NiPt) is highly catalytic for the oxygen reduction reaction (ORR) in acidic electrolytes because the dealloying process produces ligaments with a platinum-rich skin and a nickel-containing core, with this compositional variation leading to strain and ligand effects that reduce the activation barrier for ORR, analogously to nickel platinum nanoparticles.[3−8]

Nanoporous metals also provide a framework for more complex catalyst structures that derive unique benefits from reactant transport into and out of their bicontinuous porous morphology. As an example, impregnation of the pores of np-NiPt with a hydrophobic ionic liquid (IL) possessing a high oxygen solubility creates a composite catalyst whose aggregate activity when under kinetic control is increased by the ratio of the oxygen solubilities in the IL to the electrolyte.[9,10] Chen and co-workers extended this concept to make nanoframe NiPt catalysts impregnated with the specific ionic liquid [MTBD][beti], which has provided one of the highest reported ORR activity catalysts to date.[11]

Here we show that np-NiPt can also be used to create a "diffusion selective electrocatalyst", where selectivity can be tuned by controlling the relative diffusional fluxes of reactants into the nanoporous catalytic surface, specifically by creating a scenario where the flux of protons to the surface is small relative to the flux of the molecule we wish to reduce. As a model system, we are focusing on the oxygen reduction due to the relatively well-known reaction mechanism. However, we are examining ORR under unusual conditions, namely, reduction of molecular oxygen at greater than 1.5 V overpotentials (−0.4 V vs RHE) in aqueous media, i.e., under conditions where hydrogen evolves easily. We find that when the flux of oxygen from the bulk solution dominates the flux of protons, we observe apparent complete suppression of hydrogen evolution. This is obviously not of practical importance for oxygen reduction, but in principle, other small molecules, such as carbon dioxide and nitrogen, could be selectively reduced using a similar approach.

Consider the four-electron oxygen reduction reaction mechanism in acidic electrolytes,

$$O_2 + 4H^+ + 4e^- \rightarrow 2H_2O \quad (1)$$

At sufficient overpotentials in highly acidic solutions, this mechanism becomes rate-limited by diffusion of oxygen to the catalyst surface due to the abundance of protons. The inverted scenario in which ORR is proton diffusion-limited occurs in a less acidic solution, with the transition between these regimes near pH 3.0, where the concentration of protons is close to the solubility of oxygen in aqueous electrolytes, of order 1 mM.[9,10,12] In a deaerated nonporous electrode at a high

Received: October 17, 2016
Published: February 17, 2017

DOI: 10.1021/jacs.6b10855
J. Am. Chem. Soc. 2017, 139, 3663−3668

overpotential, one expects a plateau in the reduction current that is associated with diffusion-limited proton transport. This effect has recently been studied in detail by Auinger et al.[13,14] They see reactions that either consume or produce protons, or hydroxide can demonstrate drastic changes of interfacial pH, particularly at moderate pH values between 4.0 and 10.0. This was determined via mathematical modeling of the Nernst–Planck equation incorporating a generalized term for the reaction rate for hydrogen evolution reaction (HER)/Hydrogen Oxidation Reaction (HOR) to address the consumption/production of a species at the interface.

One expects more complex behavior with nanoporous electrodes in electrolytes saturated with oxygen, where there are several possible reactions, as well as multiple species for which to account. In particular, while mechanism 1 is expected to be facile, protons in the pores of the catalyst will become rapidly depleted, slowing both HER and ORR. Another possible reduction pathway for molecular oxygen produces hydrogen peroxide, but this reaction is not catalyzed by Pt surfaces[15−17] or Pt_3Ni alloys;[18] in fact, np-NiPt is more catalytically active toward the disproportionation of H_2O_2 than its planar counterpart, analogously to planar versus np-Au.[19]

Given these considerations, if proton concentrations are sufficiently depleted within the pores of the nanoporous electrode, our expectation is that oxygen will be reduced via the aprotic oxygen reduction mechanism,

$$O_2 + 2H_2O + 4e^- \rightarrow 4OH^- \quad (2)$$

The standard electrode potential for this reaction is +0.4 V vs RHE, but it has been observed primarily in alkaline solutions, where it does not compete with either HER or the traditional proton-consuming ORR mechanism shown in eq 1.[20,21] Using a nanoporous electrode in an oxygen-saturated and intermediate pH electrolyte, predicting catalytic selectivity rapidly becomes complex. There is the possibility of different reactions dominating at the outer surface of the catalytic layer and within the pores due to steep concentration gradients for all reactants, in addition to relatively slow diffusion kinetics through the pores. In this study, we attempt to elucidate the catalytic activity of np-NiPt toward the ORR in this regime, presenting this as a model system of a more general electroreduction scheme in aqueous media with a nanoporous metal catalyst possessing tunable selectivity.

EXPERIMENTAL METHODS

High surface area catalysts. Nanoporous NiPt electrodes were formed through electrochemical dealloying as previously described.[9,10] In summary, a precursor alloy with a composition of 77 at. % Ni/23 at. % Pt is machined into a 5 mm disk suitable for use in a Pine Instruments Rotating Disk Electrode (RDE), and then polished and annealed under argon. The electrode surface is dealloyed to a specified depth in the RDE by repeated cycling of the potential from 0.0−1.2 V versus RHE in 0.1 M sulfuric acid (J.T. Baker, 95−98%). The resulting np-NiPt catalyst disk contains ligaments 3−5 nm in diameter. Cyclic voltammetry of the electrode (Figure 1) is indicative of an outer surface layer comprised of Pt, whereas energy dispersive X-ray spectroscopy (EDAX) indicates that the average bulk composition contains 25 at. % residual Ni. The depth of dealloying was measured using hydrogen under potential deposition (H_{UPD}) to determine the effective surface area, which was then normalized by the geometric surface area. Except when specified otherwise, the roughness factor R_f was approximately 150 in all the experiments reported in this manuscript.

All of the ORR measurements, some of which lasted for days, did not change the cyclic voltammetry, or lead to further dealloying. As a note, the catalyst surface was physically unchanged throughout the experiments in either electrolyte solution. Figure 1 shows a representative cyclic voltammogram of the np-NiPt surface before and after performing an extended ORR experiment with no significant differences.

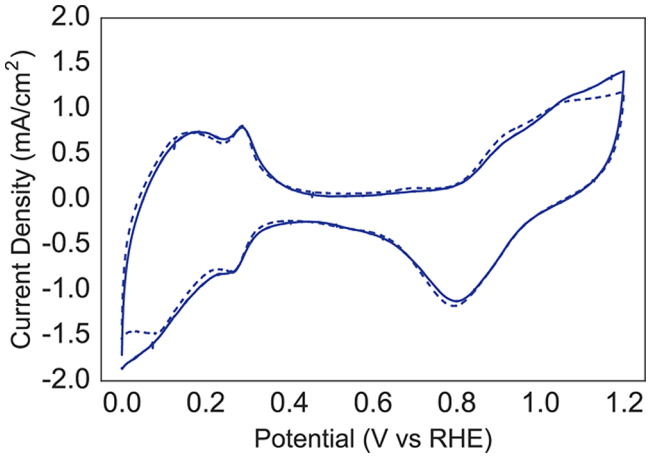

Figure 1. Cyclic voltammograms of np-NiPt before (black) and after (blue) ORR measurements in 0.1 M H_2SO_4 using a sweep rate of 5 mV/s. (Approximately 72 h of measurement.)

Chemicals. Solutions of 0.1 M sodium sulfate (Sigma-Aldrich, ACS reagent ≥99.0%, anhydrous) were buffered to the appropriate pH with 0.1 M sulfuric acid and 0.1 M sodium hydroxide (Fisher Scientific, 98.7%), measured with a Mettler-Toledo SevenExcellence pH meter. Solutions of 0.1 M potassium perchlorate (Acros Organics, 99+%) were buffered in a similar manner using 0.1 M perchloric acid (Sigma-Aldrich, 70%) and 0.1 M potassium hydroxide (Fisher Scientific, Certified ACS). Electrolytes were prepared with Millipore Milli-Q water. Glassware was cleaned by soaking in a solution of NoChromix (Godax Laboratories, Inc.) and concentrated sulfuric acid overnight.

Electrochemical measurements. Oxygen reduction activity was measured using a Gamry Interface 1000 Potentiostat and a Pine Instruments Rotating Disk apparatus. All measurements were made potentiostatically in which data points were taken every 50 mV by holding the samples at a fixed potential and then recording the steady state current, starting at more positive potentials and stepping negatively. A mercurous sulfate reference electrode (Hach Company) was used for all measurements, with potential scaled to the reversible hydrogen electrode (RHE) to account for differences in pH among solutions.

A Pine Instruments Rotating Ring Disk Assembly with a platinum ring insert (99.99%) was used for all rotating rink disk electrode (RRDE) measurements. The Pt ring electrode was generally fixed at 1.1 V vs RHE, where the oxidation of hydrogen is diffusion-limited, but any oxygen in the electrolyte will not readily reduce.

RESULTS AND DISCUSSION

We first compare catalysis behavior in deaerated and oxygen-saturated solutions to identify currents associated with HER and ORR. Figure 2 shows potentiostatic (steady-state) HER and ORR currents using np-NiPt electrocatalysts in buffered sulfate solutions. For deaerated electrolytes, the high proton concentration results in rapid hydrogen evolution below 0.0 V vs RHE at pH 1. As the pH is increased, HER becomes limited by the rate of protons reaching the catalyst surface, resulting in plateaus of current density below 0.0 V, with HER remaining the dominant reaction. The magnitude of this proton flux-limited current density decreases with the proton concentration in solution, consistent with results seen by Strmcnik et al. for strictly diffusion-limited currents.[22]

DOI: 10.1021/jacs.6b10855
J. Am. Chem. Soc. 2017, 139, 3663−3668

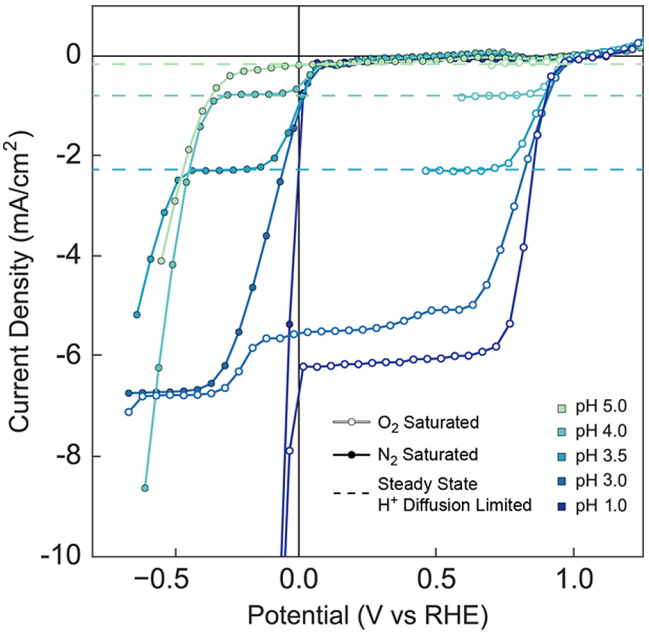

Figure 2. Differences in steady-state ORR and HER current densities as they vary with pH. (solid circles) HER current density versus the reversible hydrogen electrode (RHE) potential in N_2 saturated 0.1 M Na_2SO_4 electrolyte; (hollow circles) ORR current density versus RHE in O_2 saturated 0.1 M Na_2SO_4 electrolyte. All data were taken at 1600 rpm, sweeping from positive to negative potentials. (dashed lines) proton-diffusion-limited current densities for pH 3.5, 4.0, and 5.0.

The ORR currents are measured using the same parameters, but now in an oxygen-saturated solution. Using a Pt microdisk protocol to determine the oxygen solubility, Snyder et al.[9] found these electrolytes to have an oxygen solubility of nearly 1 mM. Assuming this value is comparable to the dilute electrolytes used here, a pH 3.0 solution will have the proton and oxygen concentrations nearly equal. Above pH 3.0, the oxygen flux is no longer the limiting species; rather the proton flux determines the reaction rate. It becomes evident from Figure 2 that the current densities for HER and ORR are equal in these higher pH solutions, because, under proton diffusion control, mechanism 1 is rate-limited by the 1-electron reduction of a proton. The general limiting current density i_{lim} in an RDE experiment is given by the Levich equation

$$i_{lim} = (0.620)nFD^{2/3}\omega^{1/2}\nu^{-1/6}C \quad (3)$$

where ω is the rotation rate of the electrode (radians/s), ν is the kinematic viscosity of the solution, F is Faraday's constant, D and C are the diffusion coefficient and concentration of species limiting the reaction, and n is the number of electrons transferred to the rate-limiting species. After performing these measurements in a deaerated solution at potentials suitable for HER at several rotation rates, we are able to determine the effective diffusion coefficient, D, for protons in a moderate pH solution: for a pH 4.0 solution of 0.1 M sodium sulfate, D_{H^+} is equal to 3.65×10^{-4} cm^2/s. This is similar to literature values of 2.13×10^{-5} cm^2/s for proton diffusion in pure water, measured by Simpson and Carr[23] using nuclear magnetic resonance free precision techniques. Using the calculated diffusion coefficient to analyze currents measured during ORR in the same pH solutions (but at positive potentials of 0.6 V; see Figure 4), Levich analysis is consistent with one electron transfer for the diffusion-limited reactant. This confirms that both rates are controlled by the diffusion of protons.

Given the facility with which np-NiPt catalyzes HER, it is surprising that when examining potentiostatic ORR currents at moderate pH (pH 4.0) over np-NiPt, we observed that ORR remains active via the proton diffusion-limited acidic mechanism to potentials as low as −0.4 mV vs RHE, as shown in Figure 3. No hydrogen evolution was observed as bubbles

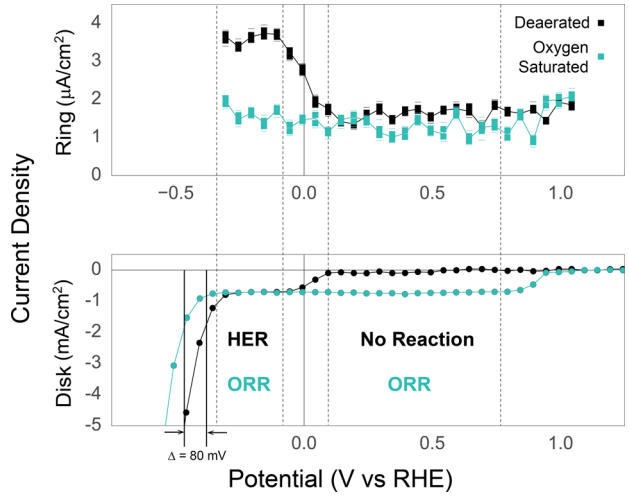

Figure 3. Potentiostatic ORR current densities and simultaneous ring current densities in 0.1 M Na_2SO_4 electrolytes at pH 4.0, under deaerated (N_2 saturated) and O_2 saturated conditions at 1600 rpm versus the disk potential. The Pt ring was held at a potential of 1.1 V vs RHE, while the np-NiPt disk was stepped negatively in potential with 16 min step holds at each potential until the current reached a steady state. Note the rise in ring current below 0.0 V vs RHE in deaerated electrolyte, indicating HOR at the ring, and that this is not observed in oxygen-saturated electrolyte. Note also the shift in the onset of water reduction in oxygen-saturated electrolyte compared to oxygen-saturated electrolyte.

during the course of the experiment, nor was any hydrogen produced that could be detected via hydrogen oxidation in a rotating ring-disk electrode (RRDE) measurement (Figure 3); in contrast, hydrogen readily evolves in the corresponding experiment in deaerated solution. These are potentiostatic experiments, wherein the current for each potential was measured after a suitable time for the current density to reach steady state. In this case some initial hydrogen evolution may occur in the transient regime, but it is fully suppressed once the current reaches a steady-state value.

Close examination of the disk current densities shown in Figure 3 reveals there is a shift in the onset potential for water reduction between the deaerated and oxygen-saturated solutions occurring near −0.5 V. When oxygen is being reduced, there is a shift of 80 mV in this onset relative to the deaerated control, corresponding to a shift in pH relative to RHE from 4.0 to 5.3. This alludes to some formation of hydroxide in the transient behavior that leads to a variation in the interface pH, a point we will return to later in this discussion.

Sodium sulfate acts as a buffer to minimize pH variations in the electrolyte, so to study whether buffering effects contribute to the suppression of hydrogen evolution, we compared the ORR results to experiments performed with a perchlorate-based electrolyte, which is much more weakly buffered. In

DOI: 10.1021/jacs.6b10855
J. Am. Chem. Soc. 2017, 139, 3663−3668

perchlorate-based solution with pH 4.0, significantly different ORR behavior was observed compared to the corresponding experiment in sulfate solution, as shown in Figure 4. At low

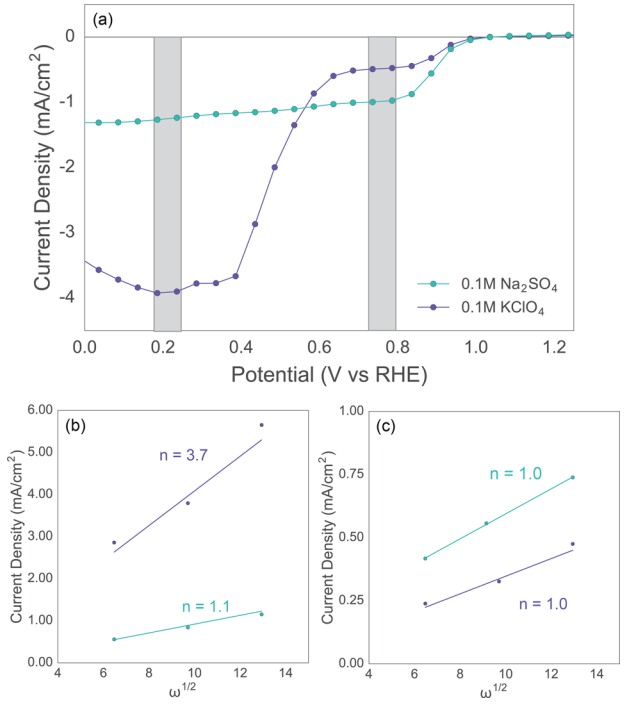

Figure 4. Comparison of electrolyte effects on ORR behavior at steady state in buffered pH 4 electrolytes (a). (b and c) Levich plots and calculated number of electrons transferred for each electrolyte at the potential ranges as marked in (a). By varying rotation rate and substituting known values for the diffusion coefficient and concentration of the limiting species, the number of electrons transferred, *n*, is calculated to determine the reaction mechanism for oxygen reduction dominating for each potential regime, dependent on the electrolyte employed.

overpotentials (from 0.6−0.9 V), both electrolytes promote proton diffusion-limited ORR (n = 1) via mechanism 1. Small variations in pH may contribute to the slight discrepancies in current densities between 0.5 and 1.0 V, but they are primarily caused by different effective diffusivities of protons in buffered vs nonbuffered electrolytes. Using the same protocol as described previously to calculate an effective D_{H^+} in sulfate-based electrolytes, we determined D_{H^+} of perchlorate-based solutions to be 1.43 × 10^{-4} cm^2/s at pH 4.0, less than half of that in sulfate solutions.

At high overpotentials, the different electrolytes showed very different behavior. Specifically, np-NiPt in perchlorate clearly exhibits a mechanism limited by 4-electron reduction of oxygen, as confirmed by the Levich equation (eq 3). Using values of C and D for the oxygen solubility and diffusivity in 0.1 M $HClO_4$ from ref 9, the calculated number of electrons transferred (n) is about $n \sim 4$. This result implies that the ORR is no longer limited by the diffusion of protons to the catalyst, but since the solution concentration of protons remains relatively unchanged, mechanism 1 can no longer explain the current density observed. We conclude that the perchlorate-based solution appears to strongly favor the proton-free oxygen reduction mechanism, eq 2, while in sulfate-based media this mechanism is not observed in steady-state measurements. This mechanistic change indicates that while activity is a property largely dictated by the catalyst, the matters of selectivity and product formation are influenced by electrolyte choice. In fact, in this extreme case there appears to be a total shift from one reaction to another caused exclusively by the electrolyte.

This is not to say mechanism 2 (proton free ORR) is never present in sulfate electrolytes; the increased shift in local pH gathered from Figure 3 illustrates the formation of hydroxide is likely in order to change the surface pH. However, by the time steady state current values are achieved, the proton free mechanism 2 is effectively switched off in the sulfate-buffered solutions, while becoming dominant in the perchlorate-based solutions. To further understand the ORR differences in strongly and weakly buffered electrolytes, it is necessary to address not only the steady-state results, but also the time-dependent evolution of the system to such an equilibrium. At short times, perchlorate and sulfate solutions appear to have identical behaviors, but it is clear from the potentiostatic measurements that the two electrolytes behave differently when the potential is held over a longer time period. The perchlorate-based system reaches steady state quite quickly with a simple exponential-type decay across the entire potential range which is associated with simple double layer charging, as shown in Figure 5 with the measured current plotted versus time. In

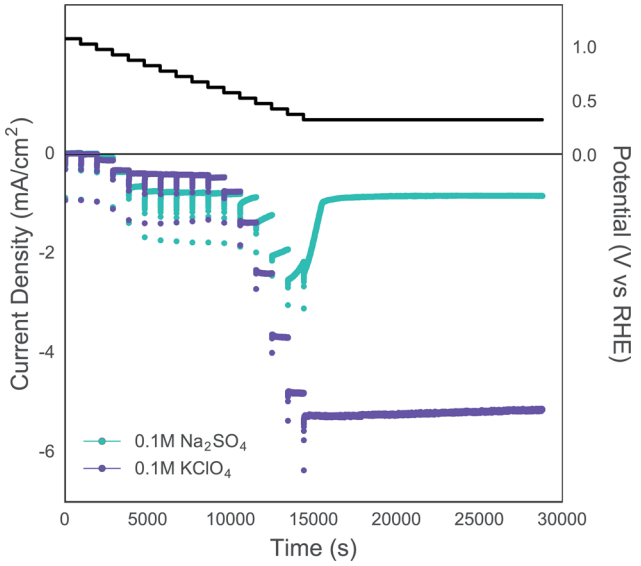

Figure 5. Potentiostatic ORR current densities in buffered 0.1 M Na_2SO_4 (green) and buffered 0.1 M $KClO_4$ (purple) electrolytes to pH 4.0 at 1600 rpm versus time. Shown in black is the potential versus the reversible hydrogen electrode (RHE) applied at each time. Note the final time step corresponds to a potential near 0.3 V vs RHE that was held for an extended time. This was done so as to ensure no complications associated with the competing HER below 0.0 V.

sulfate solution, the decay behavior is the same over the range where the ORR is dominated by the proton consuming mechanism (above 0.6 V vs RHE), but in the range where the ORR shifts the reaction mechanism in perchlorate solutions to a 4-electron reduction (below 0.6 V vs RHE), there is a longer transient in sulfate solutions that cannot be explained by double layer charging, with the current decaying slowly back to the proton-limited ORR current between several potential steps and over the course of more than an hour before reaching the final steady state behavior. Thus, when sufficient time is allowed for the transient currents to dissipate, the result is the same as

DOI: 10.1021/jacs.6b10855
J. Am. Chem. Soc. 2017, 139, 3663−3668

shown in Figure 3: proton diffusion-limited reduction of oxygen suppressing hydrogen evolution at large overpotentials.

The onset of the transient period in sulfate matches the potential where the proton-free ORR mechanism becomes operational, but we see no evidence of this mechanism at steady state, suggesting that the transient current is associated with self-limiting hydroxide-evolving ORR. The transient formation of hydroxide should drive a pH increase at the catalyst/electrolyte interface, and in sulfate we indeed see a shift in the onset for water reduction associated with a moderate rise in interface pH, as discussed above. Such a shift is not seen in the unbuffered perchlorate solution, where although proton transport is slower relatively, we expect the solution cannot sustain steep pH gradients. We do not think, however, that interface basification alone causes the difference in reaction mechanism. In fact, we would expect mechanism 2 to operate more robustly in a buffered solution, such as sulfate, where such local pH changes are mitigated, rather than in an unbuffered solution like perchlorate. Since in reality the opposite behavior is observed, it suggests the proton-free ORR mechanism (eq 2) is limited kinetically in sulfate-based media rather than strictly due to a solution buffering effect. The long duration of the transient could be associated with the porous nature of the catalyst, providing a large surface area that requires passivation before the mechanistic change takes place.

In support of the hypothesis that some passivation of the high surface area is necessary to switch mechanisms, the transient behavior shown in Figure 5 was observed only the first time a long-duration ORR experiment was run on the catalyst, with subsequent runs displaying a much shorter transient period, as shown in Figure 6. Operating the same catalyst in a strongly acidic electrolyte where the reaction is diffusion-limited by oxygen rather than protons can mitigate this behavior. After this "recovery" protocol, the transient behavior returned to that originally observed when the same catalyst was transferred back to mildly acidic sulfate solution, behaving as a new sample would for 2−3 cycles before reaching true steady state behavior. This suggests an additional control of the selectivity of the catalyst, as well as reversibility. At these high overpotentials with the electrocatalyst surface at such negative potentials, there is likely no anion adsorption. Therefore, our results point to a hypothesis that, depending on the electrolyte, the surface structure of np-NiPt might be modified. Such subtle surface modifications or reconstructions have been seen in other catalytic dealloyed metals, such as a faceting transition seen in nanoporous gold in a carbon monoxide reactant stream,[24] but to our knowledge they have not been seen in np-NiPt and warrant further investigation.

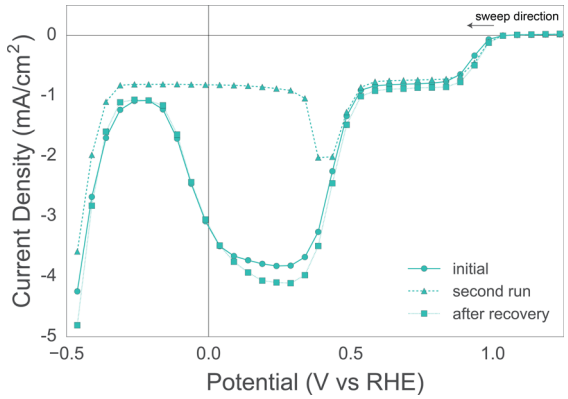

Figure 6. Transient behavior of oxygen reduction current vs potential. When ORR is measured initially in 0.1 M Na_2SO_4 electrolytes, there is a significant transient measured beginning near 0.5 V vs RHE, resulting in an apparent current wave seen until the potential drops below 0.0 V. After multiple sweeps, this transient becomes less severe and recovers to steady state much more rapidly (dashed line); eventually, this behavior is not seen at all (as in Figure 2). After holding the np-NiPt in a highly acidic 0.1 M H_2SO_4 solution at 0.25 V vs RHE for several hours, the original behavior can be recovered after this "recovery" step, as shown with the dotted line.

CONCLUSIONS

This work presents an unusual application of nanoporous electrocatalysts. While porous catalysts have been shown to have high activity for a variety of reactions similar to other metal-based electrocatalysts, the porosity itself has not been explicitly utilized. Through careful control of diffusion rates to the catalytic surface, oxygen reduction can be driven in place of hydrogen evolution in a potential regime where HER usually dominates, and on a catalyst that is also highly active for HER. Furthermore, by changing the electrolyte solution, the dominant reaction can be changed, in our case, from the acidic or alkaline mechanism for ORR. The transient behavior observed provides another interesting potential application, because the duration of the transient combined with the ability to recondition the catalyst means that reactions which occur only transiently could be performed with acceptable efficiency by cycling the electrolyte environment of the catalyst.

This collection of results opens the door for a new generation of multifunctional electrocatalysts where multiple reactions can be performed with high selectivity and excellent catalytic activity over the same catalyst surface. The strategy here is not specific to nanoporous NiPt, as many different nanoporous metals can be made from a wide variety of constituents to selectively target particular reactions. Reactions could be cycled or performed alternately in the same electrochemical system and even at the same potential by controlling the electrolyte environment and the fluxes of reactant species to the interface, and taking full advantage of the porous nature of the catalyst material. Our strategy might be particularly effective for electrochemical CO_2 reduction, for which hydrogen evolution competing with the electroreduction is endemic.

AUTHOR INFORMATION

Corresponding Author

*Jonah.Erlebacher@jhu.edu

ORCID

Ellen E. Benn: 0000-0003-2624-9245

Notes

The authors declare no competing financial interest.

ACKNOWLEDGMENTS

This work is supported by US Department of Energy under grant DE-SC0008686. Special thanks to I.M. for his superior knowledge of color schemes and endless figure critiques.

REFERENCES

(1) Erlebacher, J.; Aziz, M. J.; Karma, a; Dimitrov, N.; Sieradzki, K. *Nature* **2001**, *410* (6827), 450.

DOI: 10.1021/jacs.6b10855
J. Am. Chem. Soc. 2017, 139, 3663−3668

(2) Mccue, I.; Benn, E.; Gaskey, B.; Erlebacher, J. *Annu. Rev. Mater. Res.* **2016**, *46*, 1.
(3) Greeley, J.; Stephens, I. E. L.; Bondarenko, a S.; Johansson, T. P.; Hansen, H. a; Jaramillo, T. F.; Rossmeisl, J.; Chorkendorff, I.; Nørskov, J. K. *Nat. Chem.* **2009**, *1* (7), 552.
(4) Xin, H.; Holewinski, A.; Linic, S. *ACS Catal.* **2012**, *2* (1), 12.
(5) Nørskov, J. K.; Rossmeisl, J.; Logadottir, A.; Lindqvist, L.; Kitchin, J. R.; Bligaard, T.; Jónsson, H. *J. Phys. Chem. B* **2004**, *108* (46), 17886.
(6) Stamenkovic, V. R.; Fowler, B.; Mun, B. S.; Wang, G.; Ross, P. N.; Lucas, C. A.; Marković, N. M. *Science* **2007**, *315* (5811), 493.
(7) Stephens, I. E. L.; Bondarenko, A. S.; Perez-Alonso, F. J.; Calle-Vallejo, F.; Bech, L.; Johansson, T. P.; Jepsen, A. K.; Frydendal, R.; Knudsen, B. P.; Rossmeisl, J.; Chorkendorff, I. *J. Am. Chem. Soc.* **2011**, *133* (14), 5485.
(8) Koh, S.; Strasser, P. *J. Am. Chem. Soc.* **2007**, *129* (42), 12624.
(9) Snyder, J.; Fujita, T.; Chen, M. W.; Erlebacher, J. *Nat. Mater.* **2010**, *9* (11), 904.
(10) Benn, E.; Uvegi, H.; Erlebacher, J. *J. Electrochem. Soc.* **2015**, *162* (10), H759.
(11) Chen, C.; Kang, Y.; Huo, Z.; Zhu, Z.; Huang, W.; Xin, H. L.; Snyder, J. D.; Li, D.; Herron, J. a; Mavrikakis, M.; Chi, M.; More, K. L.; Li, Y.; Markovic, N. M.; Somorjai, G. a; Yang, P.; Stamenkovic, V. R. *Science* **2014**, *343* (6177), 1339.
(12) Battino, R.; Rettich, T. R.; Tominaga, T. *J. Phys. Chem. Ref. Data* **1983**, *12* (2), 163.
(13) Auinger, M.; Katsounaros, I.; Meier, J. C.; Klemm, S. O.; Biedermann, P. U.; Topalov, A. a; Rohwerder, M.; Mayrhofer, K. J. J. *Phys. Chem. Chem. Phys.* **2011**, *13* (36), 16384.
(14) Katsounaros, I.; Meier, J. C.; Klemm, S. O.; Topalov, A. A.; Biedermann, P. U.; Auinger, M.; Mayrhofer, K. J. J. *Electrochem. Commun.* **2011**, *13* (6), 634.
(15) Damjanovic, a.; Brusic, V. *Electrochim. Acta* **1967**, *12* (6), 615.
(16) Nenad, M.; Markovic; Gasteiger, H. a.; Ross, P. N. *J. Phys. Chem.* **1995**, *99* (11), 3411.
(17) Sepa, D. B.; Vojnovic, M. V.; Damjanovic, A. *Electrochim. Acta* **1981**, *26* (6), 781.
(18) Ferreira De Morais, R.; Franco, A. A.; Sautet, P.; Lo, D. *ACS Catal.* **2016**, *6* (9), 5641.
(19) Zeis, R.; Lei, T.; Sieradzki, K.; Snyder, J.; Erlebacher, J. *J. Catal.* **2008**, *253* (1), 132.
(20) Gasteiger, H. a; Ross, P. N. *J. Phys. Chem.* **1996**, *100* (16), 6715.
(21) Ramaswamy, N.; Mukerjee, S. *Adv. Phys. Chem.* **2012**, *2012*, 1.
(22) Strmcnik, D.; Uchimura, M.; Wang, C.; Subbaraman, R.; Danilovic, N.; van der Vliet, D.; Paulikas, A. P.; Stamenkovic, V. R.; Markovic, N. M. *Nat. Chem.* **2013**, *5* (4), 300.
(23) Simpson, J. H.; Carr, H. Y. *Phys. Rev.* **1958**, *111* (5), 1201.
(24) Fujita, T.; Guan, P.; McKenna, K.; Lang, X.; Hirata, A.; Zhang, L.; Tokunaga, T.; Arai, S.; Yamamoto, Y.; Tanaka, N.; Ishikawa, Y.; Asao, N.; Yamamoto, Y.; Erlebacher, J.; Chen, M. *Nat. Mater.* **2012**, *11* (9), 775.

DOI: 10.1021/jacs.6b10855
J. Am. Chem. Soc. 2017, 139, 3663−3668